



Since January 2020 Elsevier has created a COVID-19 resource centre with free information in English and Mandarin on the novel coronavirus COVID-19. The COVID-19 resource centre is hosted on Elsevier Connect, the company's public news and information website.

Elsevier hereby grants permission to make all its COVID-19-related research that is available on the COVID-19 resource centre - including this research content - immediately available in PubMed Central and other publicly funded repositories, such as the WHO COVID database with rights for unrestricted research re-use and analyses in any form or by any means with acknowledgement of the original source. These permissions are granted for free by Elsevier for as long as the COVID-19 resource centre remains active.



Potential of antibody pair targeting conserved antigenic sites in diagnosis of SARS-CoV-2 variants infection

Siling Wang^{a,1}, Yangling Wu^{b,1}, Yizhen Wang^{a,1}, Zihao Chen^a, Dong Ying^a, Xue Lin^a, Chang Liu^a, Min Lin^a, Jinlei Zhang^a, Yuhe Zhu^a, Shaoqi Guo^a, Huixian Shang^a, Xiuting Chen^a, Hongsheng Qiang^a, Yifan Yin^a, Zimin Tang^{a,*}, Zizheng Zheng^{a,*}, Ningshao Xia^{a,*}

^a State Key Laboratory of Molecular Vaccinology and Molecular Diagnostics, National Institute of Diagnostics and Vaccine Development in Infectious Diseases, School of Public Health, School of Life Sciences, Xiamen University, 361102 Xiamen, Fujian, PR China

^b Emergency Department, The First Affiliated Hospital of Xiamen University, 361003 Xiamen, Fujian, PR China

ARTICLE INFO

Keywords:

COVID-19
SARS-CoV-2
Spike antigen
ELISA
Antibody pair

ABSTRACT

Coronavirus disease 2019 (COVID-19) caused by SARS-CoV-2 has become disaster for human society. As the pandemic becomes more regular, we should develop more rapid and accurate detection methods to achieve early diagnosis and treatment. Antigen detection methods based on spike protein has great potential, however, it has not been effectively developed, probably due to the torturing conformational complexity. By utilizing cross-blocking data, we clustered SARS-CoV-2 receptor binding domain (RBD)-specific monoclonal antibodies (mAbs) into 6 clusters. Subsequently, the antigenic sites for representative mAbs were identified by RBDs with designed residue substitutions. The sensitivity and specificity of selected antibody pairs was demonstrated using serial diluted samples of SARS-CoV-2 S protein and SARS-CoV S protein. Furthermore, pseudovirus system was constructed to determine the detection capability against SARS-CoV-2 and SARS-CoV. 6 RBD-specific mAbs, recognizing different antigenic sites, were identified as potential candidates for optimal antibody pairs for detection of SARS-CoV-2 S protein. By considering relative spatial position, accessibility and conservation of corresponding antigenic sites, affinity and the presence of competitive antibodies in clinical samples, 6H7–6G3 was rationally identified as optimal antibody pair for detection of both SARS-CoV-2 and SARS-CoV. Furthermore, our results showed that 6H7 and 6G3 effectively bind to SARS-CoV-2 variants of concern (VOCs). Taken together, we identified 6H7–6G3 antibody pair as a promising rapid antigen diagnostic tool in containing COVID-19 pandemic caused by multiple VOCs. Moreover, our results also provide an important reference in screening of antibody pairs detecting antigens with complex conformation.

1. Introduction

The COVID-19 pandemic, caused by SARS-CoV-2 infection, has spread across the globe, posing a major economic and health threat to many countries (Lan et al., 2020; Poland et al., 2020; Wu et al., 2020; Zhou et al., 2020; Zhu et al., 2020). SARS-CoV-2 variants are being continuously reported, these variants of concern (VOC) present new challenges for the efficacy of approved mAb therapies or vaccines (Cerutti et al., 2021; Korber et al., 2020; McCallum et al., 2021). The primary tools for limiting the spread of COVID-19 are diagnosis, surveillance and quarantine (Lee, Chiew, and Khong, 2020). Therefore, it is urgent to develop easy-to-use, highly accurate and broad methods for

rapid identification and isolation of infected individuals. Although reverse transcription-polymerase chain reaction (RT-PCR), based on detection of SARS-CoV-2 RNA, is the current gold standard for detection of SARS-CoV-2 infection, this method represents some troublesome issues, including being time-consuming, requirement of specific and expensive machinery, and necessary of lab facilities with higher biosafety level, which hinder its application in point-of care testing (POCT) at home or in the community and high-throughput routine screening (Barnes et al., 2020; Ben-Ami et al., 2020; Li et al., 2020; Mavrikou et al., 2020; Relova et al., 2018; Wen et al., 2015; Xie et al., 2020; Zafrullah et al., 2004). Therefore, it is critical demand for rapid and accurate detection methods for SARS-CoV-2 as supplementary

* Corresponding authors.

E-mail addresses: zimintang@xmu.edu.cn (Z. Tang), zhengzizheng@xmu.edu.cn (Z. Zheng), nsxia@xmu.edu.cn (N. Xia).

¹ These authors contributed equally.

detection methods. Antigen detection with the advantages of being convenient, rapid and reliable will play a key role in COVID-19 prevention and control. Accordingly, many antigen diagnostic kits with stability and accuracy were developed, some of which are now commercially available for detection of SARS-CoV-2 infection.

The ~30 kb RNA genome of SARS-CoV-2 encodes four structural proteins including membrane (M), envelope (E), nucleocapsid (N) and spike (S) proteins. The S protein is composed of S1 and S2, the former comprising receptor binding domain (RBD) and N-terminal domain (NTD), which forms a prominent homologous trimer (Kim et al., 2020; Walls et al., 2020). Most of the commercial diagnostic kits based on antigen detection target N protein, however, some reports suggest a potential for false positive results when performing rapid detection by antigen kits targeting N protein (https://www.cdc.gov/coronavirus/2019-ncov/lab/resources/antigen-tests-guidelines.html#anchor_1597523027400). Targeting another structural protein may be a better solution. As S protein recognizes corresponding receptors, ACE2 and AXL, through RBD and NTD, thus initiating the entry process of virions into cells, S protein plays a direct role in the infection of host cells (Lan et al., 2020; Wang et al., 2021a). Therefore, there is an obvious correlation between S protein and SARS-CoV-2 infectivity, suggesting that this protein may be a direct and important marker for detection of SARS-CoV-2 infection. Furthermore, RBD domain shows obvious fewer glycosylation sites compared with the remaining domains, making it a more detectable domain (Watanabe et al., 2020). The S1, in which RBD domain is located, is easy to shed, thus further enhancing RBD detectability (Piccoli et al., 2020; Zhang et al., 2020). Despite the advantages mentioned above, the development of detection methods based on S protein is still fraught with difficulties, putatively resulted from the complex conformation of S protein. As determined by cryo-electron microscopy, pre-fusion S trimer of intact SARS-CoV-2 virions have three class of conformation, suggesting that RBD undergoes conformational movement to engage host-cell receptor ACE2 for entry into host cells (Rogers et al., 2020; Wrapp et al., 2020). Additionally, continuous emergence of SARS-CoV-2 VOCs generates serious threats to detection kits based on S protein, especially B.1.1.529 (Omicron) variant that showed significant resistance to the approved vaccines and therapeutic antibodies by alarming 15 mutations in RBD key epitopes (Cameroni et al., 2022; Cao et al., 2022). Hence, to identify optimal and broad antibodies for SARS-CoV-2 S protein detection, it becomes indispensable to comprehensively consider characteristics of the antigenic sites.

In this study, characteristics of 40 monoclonal antibodies (mAbs) targeting SARS-CoV-2 RBD, which were isolated from convalescent COVID-19 patients, were described including binding activity, conserved property and accessibility of antigenic sites, and even dominance in an immune response. Finally, 6H7–6G3 antibody pair were determined as optimal in rapid and accurate detection of SARS-CoV-2 infection, which showed high sensitivity not only in detection of SARS-CoV-2 S protein and SARS-CoV S protein, but also in detection of SARS-CoV-2 pseudovirus and SARS-CoV pseudovirus. In addition, 6H7 and 6G3 recognized conserved antigenic sites between SARS-CoV-2 and SARS-CoV, which indicates that 6H7–6G3 antibody pair may have potential in defeating the diagnostic risk posed by VOCs. Furthermore, this screening process of antibody pairs targeting transmembrane spike protein also provides an important reference for other enveloped virus with complex conformational antigens in screening detective antibody pairs.

2. Materials and methods

2.1. Recombinant expression of SARS-CoV S protein, SARS-CoV-2 S protein and RBD

A gene encoding the ectodomain of a prefusion conformation-stabilized SARS-CoV-2 S protein was synthesized, composed of SARS-CoV-2 gene sequence (residue1–1208) [GenBank accession number

MN908947.3], a C-terminal T4 fibrin trimerization motif, a HRV3C protease and 8xHisTag. Similarly, gene of SARS-CoV S protein comprised SARS-CoV gene sequence (residue1–1208) [GenBank accession number ABF65836.1], a C-terminal T4 fibrin trimerization motif, a HRV3C protease and 8xHisTag. Moreover, to express SARS-CoV-2 mutate and wildtype RBD, residues 319–541 fused to mouse IgG1 Fc domain. Recombinant expressions of these proteins were performed by the ExpiCHO™ expression system (Thermo Scientific, A29133). Briefly, plasmids encoding targeted proteins were transiently transfected into ExpiCHO cells by using ExpiFectamine™ CHO transfection kit (Thermo Scientific, A29129). The cell-free supernatants were obtained 5–7 days after transfection by centrifugation and filtration with a 0.22 µm filter. Subsequently, the proteins were purified by Ni Sepharose Excel resin, and stored in the PBS buffer.

2.2. Expression of antibody

The paired heavy and light chains were then cloned into expression vectors containing the constant regions of human IgG1 and light chain. The paired heavy and light chain expression cassettes were then transiently co-transfected into ExpiCHO cells with equal amounts of plasmids according to the manufacturer's instructions (Life Technologies), and antibodies were purified from culture supernatant 5–7 days after transfection, using a recombinant protein-A column (GE Healthcare).

2.3. Construction of SARS-CoV-2 pseudovirus and SARS-CoV pseudovirus

In order to construct the VSV pseudovirus carrying the SARS-CoV-2 spike protein, the spike gene (GenBank: MN908947) was codon optimized for expression in human cells, and the spike gene of SARS-CoV-2 with 18 amino acids truncated at the C-terminal was cloned into the eukaryotic expression vector pCAG to obtain pcag-ncovsde18. The plasmid pCAG-nCoVsd18 was transfected into Vero-E6. VSVdG-EGFP-G (Addgene, 31842) virus was inoculated into cells expressing SARS-CoV-2 Sde18 truncated protein and incubated for 1 h. Then the VSVdG-EGFP-G virus was removed from the supernatant and anti-VSV-G rat serum was added to block the remaining VSVdG-EGFP-G infection. The progeny virus will carry SARS-CoV-2 Sde18 truncated protein. After VSVdG-EGFP-G infection, supernatant was collected, centrifuged and filtered (Millipore, SLHP033RB) to obtain the SARS-CoV-2 pseudovirus without debris. SARS-CoV pseudovirus was constructed by the same method. Finally, pseudovirus was stored for use at –80 °C.

2.4. Binding activity assay

The binding activity of the mAbs against SARS-CoV S protein and SARS-CoV-2 S protein and RBD were determined using an indirect ELISA. The serially diluted mAbs were added to antigen-coated micro-well plates, and incubated at 37 °C for 30 min. Then, incubation of HRP-conjugated anti-human antibody at 37 °C for 30 min to detect the bound mAbs, followed by washing five times. Finally, substrate solution was added to the wells for 15 min at 37 °C, and reaction was stopped by adding an equal volume of stop solution (0.2 M H₂SO₄). The optical density (OD) was measured at 450 nm with a reference wavelength of 630 nm. The EC₅₀ values of the mAbs binding to specific proteins were calculated from binding curves (GraphPad Prism).

To investigate the critical residues, mAbs were conjugated with horse radish peroxidase (HRP) according to the manufacturer's instruction (Abcam, ab102890). Microwell plates were pre-coated with mutate SARS-CoV-2 RBD and wildtype SARS-CoV-2 RBD at 100 ng per well. The serially diluted mAbs-HRP were added at selected dilutions, at which OD readings was ~1.5 for wildtype RBD, and incubated at 37 °C for 30 min followed by washing five times. Substrate solution was incubated for 15 min at 37 °C, and stopped by 50 µL of 2 M H₂SO₄. Finally, OD at 450 and 630 nm were acquired. The curves between OD and protein amount

were fitted using GraphPad Prism, and area under curve (AUC) was calculated. The mutated residues were determined as critical residues for mAbs, if the reduction of binding activity calculated by $(AUC_{\text{wild}} - AUC_{\text{mutated}}) / AUC_{\text{wild}}$ was more than 75 %.

2.5. Competition-binding assay by ELISA and cluster analysis

Briefly, the unlabeled mAbs (50 μg per well) or PBS were added to RBD-coated 96-well microplates and then incubated for 30 min at 37 °C. Next, HRP-conjugated mAbs were added at selected dilutions, at which OD readings were ~ 1.5 with PBS present. After incubation for 30 min at 37 °C, the microplates were rinsed and the color was developed. The competitive ability was measured quantitatively by comparing OD in the presence or absence of competitor mAbs, and transformed using the formula $\log_2(\text{OD}_{\text{inhibited}} / \text{OD}_{\text{original}})$. For mAbs to be clustered by competitive ability, clustering distance was calculated by Euclidean, and cluster by ward.D2 method, using pheatmap R package (version: 1.0.12).

2.6. Detection of coronavirus S protein and coronavirus pseudovirus using the sandwich ELISA

Sandwich ELISA was established by coating 96-well plates with capture antibody and using HRP-conjugated detection antibody for detection. Briefly, the sample of recombinant S protein or pseudovirus was serially twofold diluted for evaluation of detection capacity of antibody pairs, then 100- μL aliquot of diluted samples was incubated at 37 °C for 30 min in the wells coated with 200 ng of capture antibody. Following five rinses with wash buffer (PBS containing 0.5 % (w/v) Tween 20 PBST), a 100- μL aliquot of capture antibody-HRP solution was added directly in each well and was incubated at 37 °C for 30 min. Based on tetramethylbenzidine substrate solution incubated at 37 °C for 15 min, absorbance reading was measured using a microplate reader (Autobio, Zhengzhou, China) at 450 nm and at 630 nm as reference. The EC50 values of antibody pairs detecting specific proteins were calculated from binding curves using GraphPad Prism.

2.7. Statistical analysis

To compare continuous variables, the unpaired *t*-test was performed. Linear regression models and Pearson correlation tests were used for correlation analyses. For difference analysis, *p* values less than 0.05 are considered statistically significant. GraphPad Prism version 8.0.1 was used for all statistical calculations.

3. Results

3.1. Confirmation of candidate antibodies for screening optimal antibody pairs

40 mAbs targeting SARS-CoV-2 RBD protein were obtained from convalescent COVID-19 patients (Wang et al., 2021b). It is known that successful detection of the target antigen by sandwich enzyme linked immunosorbent assay (ELISA) requires the optimal antibody pairs consisting the capture antibody and detection antibody, which should target different antigenic sites. To this end, competition-binding assay using ELISA were performed, and mAbs were classified into 6 clusters according to the competitive ability (Fig. S1 and S2A). 6 representative antibodies were singled out from these clusters due to high binding activity to SARS-CoV-2 S protein, majority of which bind to SARS-CoV-2 S protein with potent affinity ($\text{EC}_{50} < 100 \text{ ng/mL}$) (Fig. S2B). As 6H7, 6G3 and 4D10 showed cross-reactivity with SARS-CoV S protein, these mAbs raise the important possibility in the diagnostic platform to detect both S protein of SARS-CoV-2 and that of SARS-CoV (Fig. S2C). Above all, these results provided candidate antibodies to form antibody pairs for constitution of a successful diagnostic platform for the detection of

SARS-CoV-2 S protein and even SARS-CoV S protein.

3.2. Identification of optimal antibody pairs for detection of SARS-CoV-2 S protein and SARS-CoV S protein

The sandwich ELISA was established by coating microtiter plate with naked antibodies and using HRP (horseradish peroxidase)-conjugated antibodies for detection. To determine optimal antibody pairs, 6 candidate antibodies were matched with each other to evaluate the detection capability of SARS-CoV-2 and SARS-CoV S protein. For detection of SARS-CoV-2 S protein, 6H7 was identified as the antibody with the strongest capability to capture SARS-CoV-2 S protein (Fig. 1A and C). Based on 6H7 as a capture antibody (6H7-capture), 6G3 and 5C6 showed potent detection capability for SARS-CoV-2 S protein (Fig. 1A and C). As mentioned above, 6G3, 4D10 and 6H7 bind to both SARS-CoV-2 S protein and SARS-CoV S protein by recognizing the conserved antigenic sites. Therefore, antibody pairs formed by these antibodies may be used for detection of SARS-CoV S protein. However, just sandwich ELISA with 6H7 as capture antibody and 6G3 (or 4D10) as detection antibody can detect SARS-CoV S protein with high sensitivity (Fig. 1B and D). Taken together, these results determined the optimal antibody pairs, 6H7 antibody as capture molecule and 5C6 as detection molecule (6H7–5C6 pair) for detection of SARS-CoV-2 S protein, and 6H7 antibody as capture molecule and 6G3 as detection molecule (6H7–6G3 pair) for detection of both SARS-CoV-2 S protein and SARS-CoV S protein.

3.3. Sensitivity and specificity of 6H7-based sandwich ELISA

The sandwich ELISA was established using 6H7 antibody as capture molecule and HRP-conjugated 6G3 (or 5C6) to detect SARS-CoV-2 S protein or SARS-CoV S protein. To investigate the detection capability of the 6H7-based sandwich ELISA, serially diluted samples of SARS-CoV-2 S protein and SARS-CoV S protein were tested to perform the sensitivity analysis (concentration range of S protein: 500.00 ng/mL–59.50 fg/mL). For detection of SARS-CoV-2 S protein, the results showed that the optical density decreased gradually accompanied by reduction in concentration of SARS-CoV-2 S protein, and even if trace amounts of SARS-CoV-2 S protein were present, the signal of optical density was still detected by 6H7-based sandwich ELISA (Fig. 2A and B). In addition, no false-positive signals were observed in any negative controls, and limit of detection (LOD) was calculated as mean value of negative control plus 3 times standard deviation. The detection sensitivity was obviously improved, even only 957.00 fg/mL (95.70 fg/reaction) of SARS-CoV-2 S protein was detectable by 6H7–6G3 pair or by 6H7–5C6 pair, which has a great potential in promotion the level of SARS-CoV-2 S protein detection in point-of-care or laboratory settings (Fig. 2A). As mentioned above, the 6H7–6G3 pair can also be utilized to detect the presence of SARS-CoV S protein in samples, and even if only 30.52 pg/mL (3.05 pg/reaction) of SARS-CoV S protein was input into the sample, the optical density was still stronger than the corresponding LOD, revealing that 6H7–6G3 pair plays an important role in the detection of not only SARS-CoV-2 S protein but SARS-CoV S protein (Fig. 2B).

Sandwich ELISA by antibody pairing is an essential method to determine the content of S protein in recombinant S protein samples. By linear correlation analysis of S protein concentration and corresponding signal of optical density, the linear range of S protein detection is calculated, which is an important index to measure the quantitative capability of sandwich ELISA for S protein of SARS-CoV-2 and that of SARS-CoV. A wide linear range with high sensitivity can not only ensure sensitivity of detection and quantitative accuracy, but also avoid the waste of high concentration samples. 6H7–5C6 pair showed wide linear range from nanogram per milliliter to pique per milliliter for detection of SARS-CoV-2 S protein, as well as 6H7–6G3 pair (Fig. 2C). In addition, although 6H7–6G3 pair also sensitively detected SARS-CoV S protein, this antibody combination showed much smaller range of linear

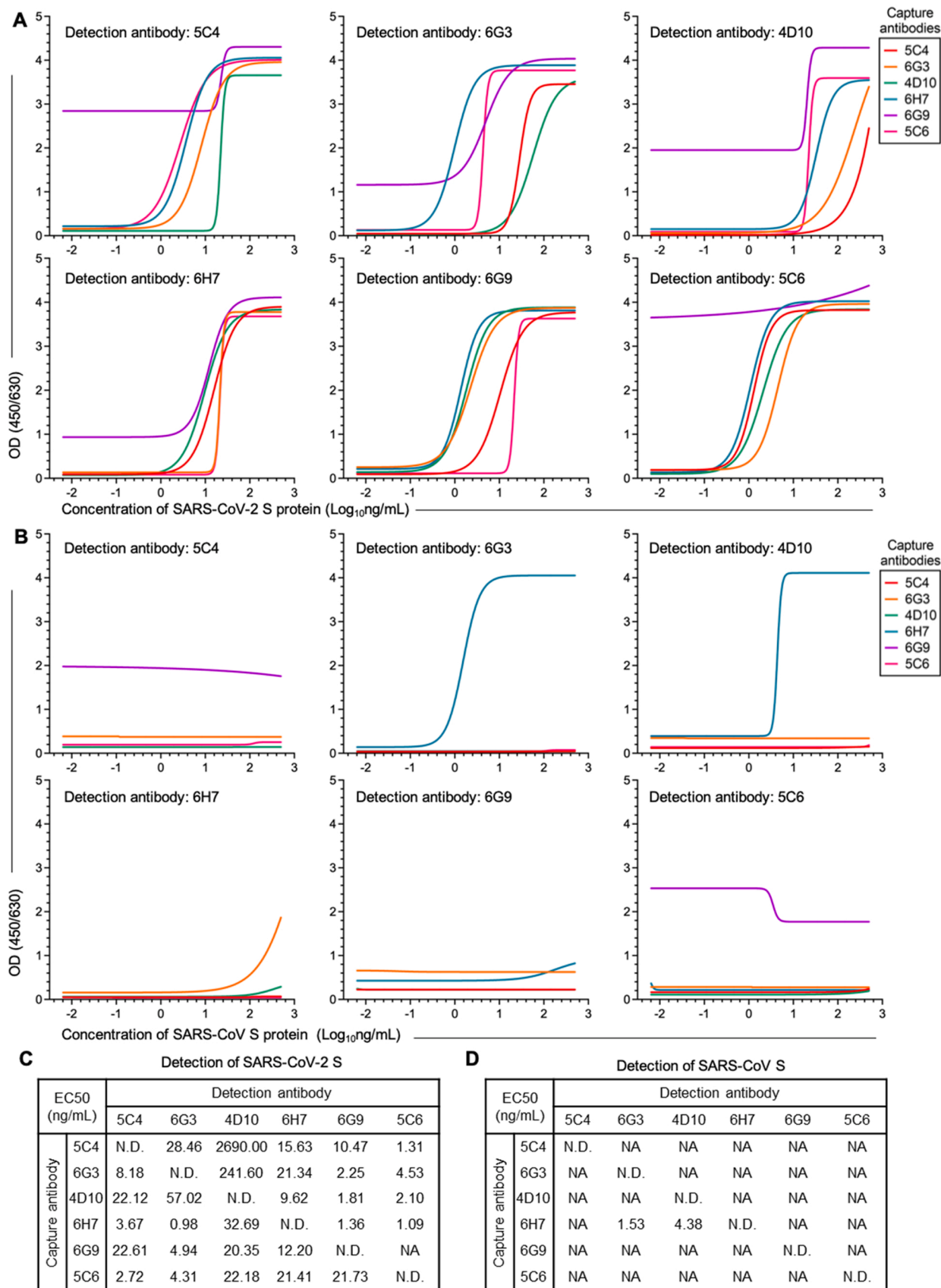


Fig. 1. Identification of antibody pair for detection of SARS-CoV and SARS-CoV-2 S protein. (A and B) Detection capacity of SARS-CoV-2 S protein and SARS-CoV S protein for 30 antibody pairs were determined by serially diluted recombinant S proteins with 500 ng/mL initial concentration. (C and D) EC50 of capture antibody–detection antibody pairs for detection of SARS-CoV and SARS-CoV-2 S protein are shown. The EC50 was analyzed by nonlinear regression (four-parameter).

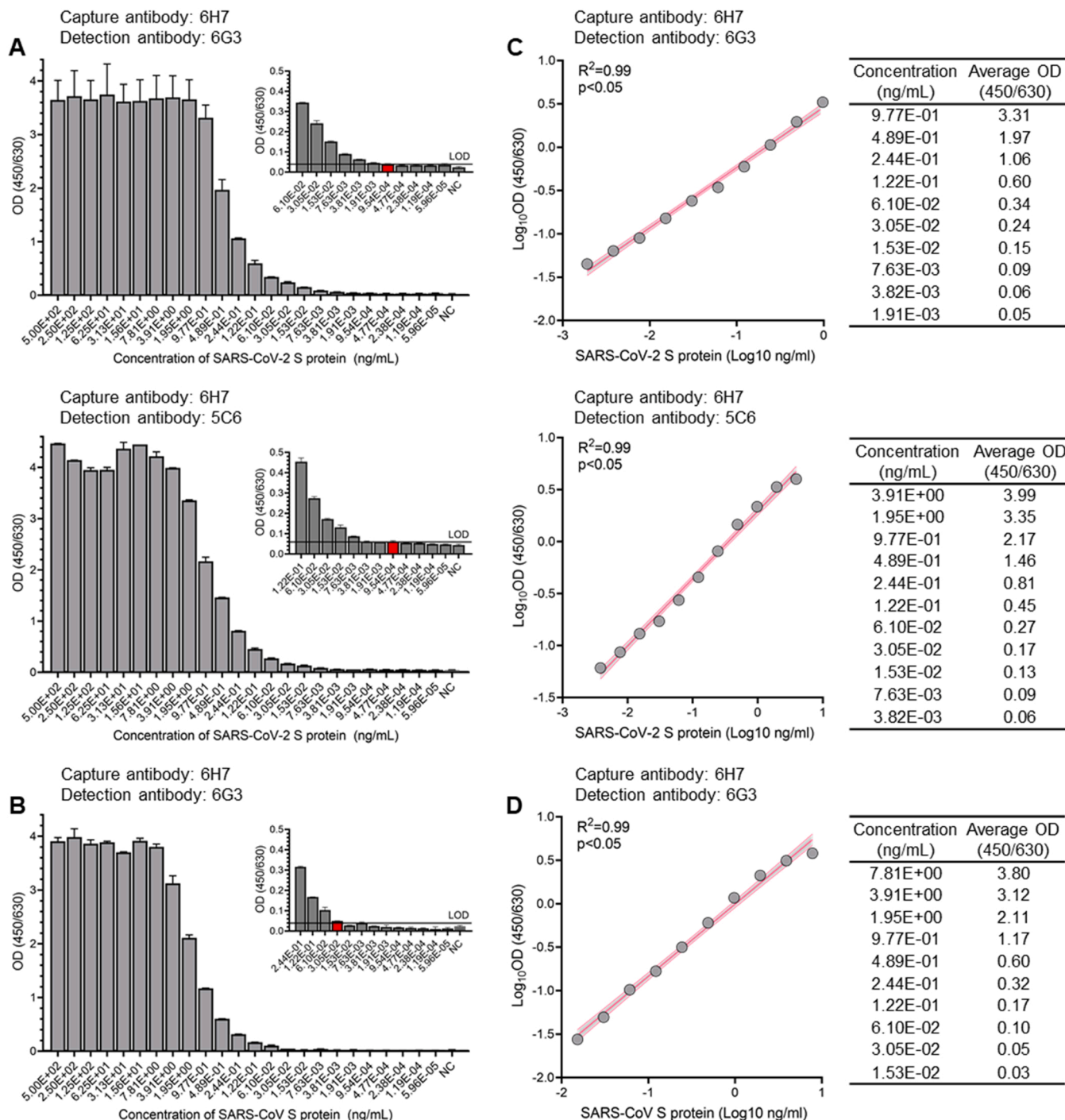


Fig. 2. Sensitivity for detection of SARS-CoV-2 S protein and SARS-CoV S protein by 6H7-based antibody pairs. (A and B) By serially diluted recombinant S protein, the sensitivity of sandwich ELISA (6H7-based) for detection of SARS-CoV-2 S protein and that of SARS-CoV S protein was determined. In the inset, red bar graphs indicate the lowest concentration that can be detected. LOD (limit of detection) was calculated by the mean value of negative controls plus three times the standard deviation. (C and D) The standard curves of sandwich ELISA (6H7-based) for detection of SARS-CoV-2 S protein and SARS-CoV S protein were established using serially diluted recombinant S protein. Curves were fitted for linear regression using GraphPad Prism software. P value and R^2 are presented.

correlation for detection of SARS-CoV S protein than for detection of SARS-CoV-2 S protein (Fig. 2D). Overall, as similar as 6H7-5C6 pair, 6H7-6G3 pair showed obviously sensitivity and quantitative capability in detection of SARS-CoV-2 S protein by sandwich ELISA method, and 6H7-6G3 pair also plays an import role in detection of SARS-CoV S protein.

Then, detection specificity was determined using MERS S1 protein, HKU1 S1 protein and respiratory syncytial virus (RSV) F protein, which

were diluted at four different concentrations (2.50×10^2 ng/mL, 3.91×10^0 ng/mL, 6.10×10^{-2} ng/mL, 9.54×10^{-4} ng/mL). For 6H7-6G3 pair, the SARS-CoV-2 S protein was successfully detected at low concentration of 9.54×10^{-4} ng/mL, however, other antigens were not detected, even at a high concentration (Fig. 3A). 6H7-5C6 pair showed similar detection specificity (Fig. 3B). Thus, the optimal antibody pairs can detect SARS-CoV-2 S protein or SARS-CoV S protein with high sensitivity and avoid cross-reactivity with other antigens.

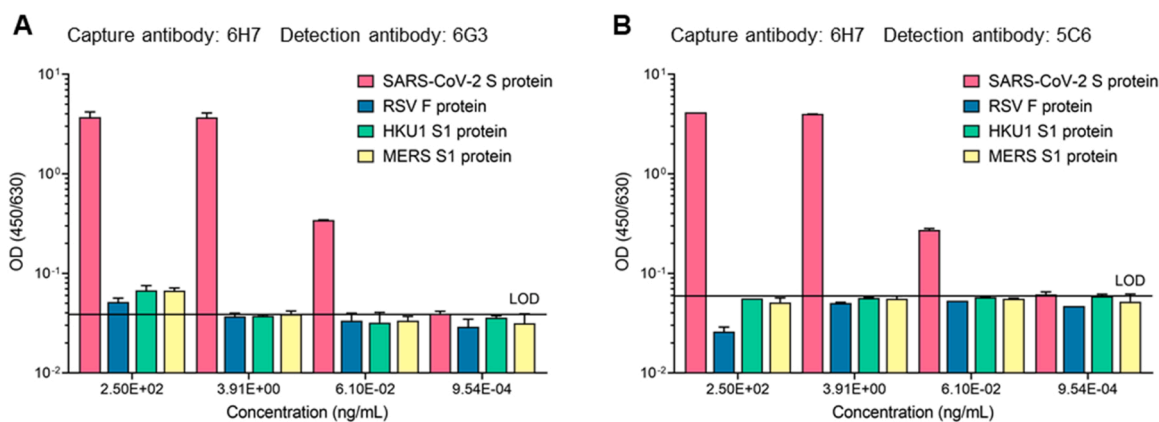


Fig. 3. Specificity for detection of SARS-CoV-2 S protein by 6H7-based antibody pairs. (A and B) By serially diluted recombinant S protein, the sensitivity of sandwich ELISA (6H7-based) for detection of SARS-CoV-2 S protein and that of SARS-CoV S protein was determined. In the inset, red bar graphs indicate the lowest concentration that can be detected. LOD (limit of detection) was calculated by the mean value of negative controls plus three times the standard deviation.

3.4. Confirmation of detection capability using SARS-CoV-2 pseudovirus and SARS-CoV pseudovirus

The isolation and culture of SARS-CoV-2 have to be handled in biosafety level-3 facilities, and it is difficult to isolate SARS-CoV from infected patient due to the disappearance of SARS-CoV infection, which limit the development of vaccine and diagnostic method. Therefore, pseudotyped VSV (vesicular stomatitis virus) carrying the S protein of SARS-CoV-2 or that of SARS-CoV was used for further confirmation of detection sensitivity for 6H7-based ELISA (Xiong et al., 2020), and results are presented in Fig. 4. The limits of detection for 6H7–6G3 pair were 1.95×10^5 copies/mL of the cultured SARS-CoV-2 pseudovirus and 3.91×10^5 copies/mL of the cultured SARS-CoV pseudovirus (Fig. 4A and B). Although detection sensitivity of SARS-CoV-2 S protein for 6H7–5C6 pair is comparable, 5C6-detection can detect SARS-CoV-2 pseudovirus at lower concentration, 4.88×10^4 copies/mL (Fig. 4A). Furthermore, the detection specificity was determined using diluted SARS-CoV-2 pseudovirus, SARS-CoV pseudovirus and RSV (Fig. 5A and B). The optical density of RSV is significantly lower than that of SARS-CoV-2 pseudovirus and SARS-CoV pseudovirus, and RSV was not detected even at high concentration of 2.50×10^7 copies/mL, revealing that 6H7-based antibody pairs might have ability to avoid occurrence of false positive in detection of clinical samples. Above all, 6H7-based

sandwich ELISA showed high detection sensitivity of S protein and will be helpful to detect the S protein of SARS-CoV-2 or that of SARS-CoV for clinical samples.

3.5. Molecular mechanism for remarkable and broad detection performance of these two antibody pairs

Next, we sought to determine the molecular mechanism of remarkable detection performance for the optimal antibody pairs. The antigenic sites recognized by each representative mAbs were determined using mutated SARS-CoV-2 RBD. The critical residues of representative mAbs were identified, N487 residue for 5C4, K378, G413, G417, Y449 and E493 residues for 6G3, K378 residue for 4D10, K462 residue for 6H7, Y449 residue for 6G9 and K444 for 5C6 (Fig. S3). Notably, the antigenic site recognized by 6H7 is to the side of RBD and away from the other antigenic site (Fig. 6A). Although just one critical residue was identified for 5C4, the antigenic site targeted by 5C4 was speculated reliably, due to the same variable region germline of heavy chain, VH3–53, playing an important role in the binding affinity to RBD by conserved binding mode, as previously reported (Yuan et al., 2020). The antigenic sites for 5C4, 6G3 and 4D10 partially overlap with each other, suggesting that these antibodies could not be paired for efficient detection of S protein due to likely steric hindrance (Fig. 6A). In addition, antigenic sites

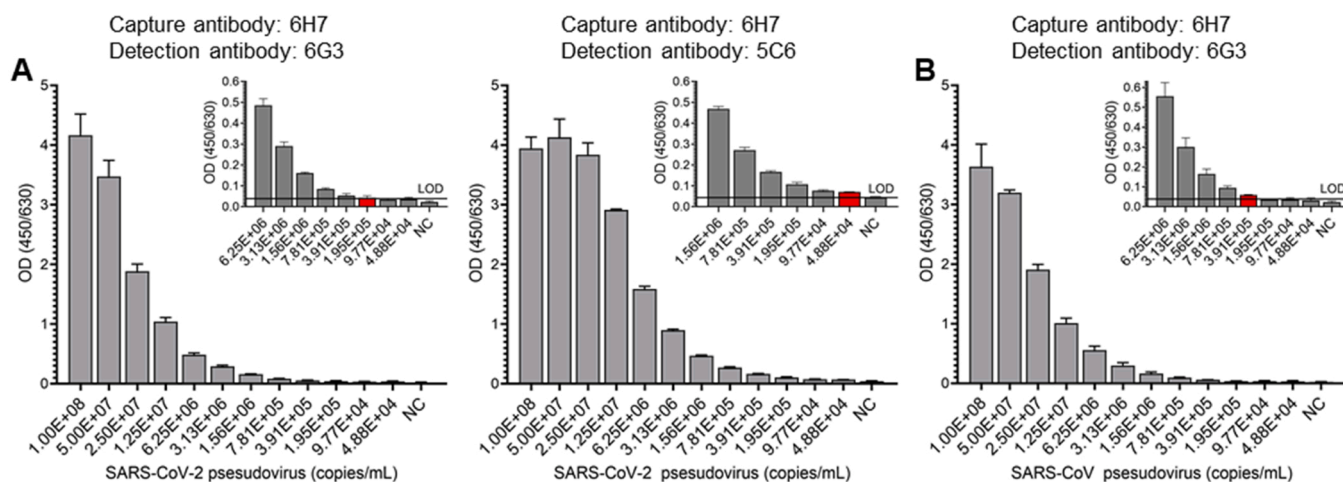


Fig. 4. Detection sensitivity of 6H7-based antibody pairs for SARS-CoV-2 and SARS-CoV. SARS-CoV-2 pseudovirus (A) and SARS-CoV pseudovirus (B) were constructed and serially diluted (concentration range: 1.00×10^8 copies/mL to 4.88×10^4 copies/mL) for determination of detection sensitivity of sandwich ELISA (6H7-based). In the insets, the lowest concentration that can be detected is marked by red bar graph. Limit of detection (LOD) was calculated by the mean value of negative controls (NC) (0 copies/mL of virus) plus three times the standard deviation.

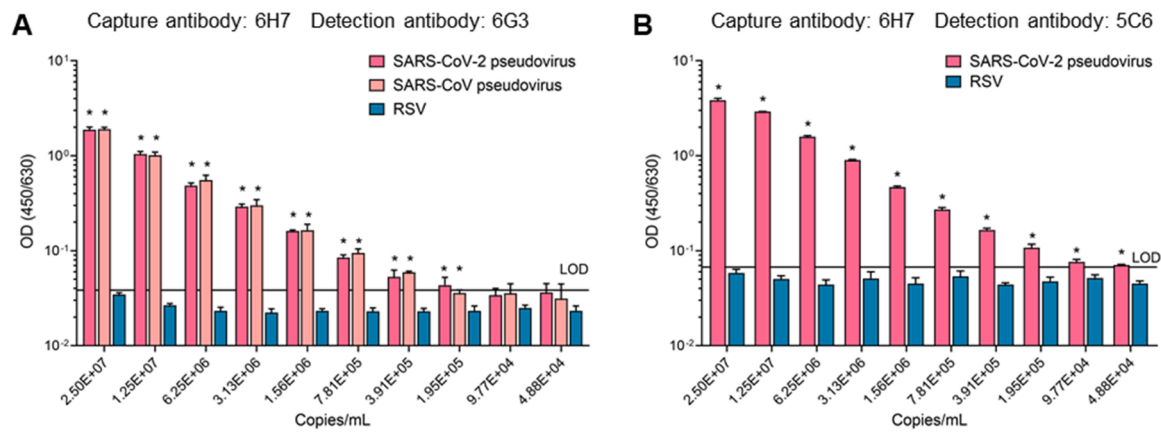


Fig. 5. Detection specificity of 6H7-based antibody pairs. By SARS-CoV-2 pseudovirus and SARS-CoV pseudovirus, detection specificity for optimal antibody pairs was determined, including 6H7-capture and 6G3-detection (A) and 6H7-capture and 5C6-detection (B). Respiratory syncytial virus (RSV) was also tested as control. Limit of detection (LOD) was calculated by the mean value of negative controls (0 copies/mL of virus) plus three times the standard deviation. The optical density of SARS-CoV-2 pseudovirus (or SARS-CoV pseudovirus) and that of RSV were compared by t test using GraphPad Prism 8.3.0. * indicates p value less than 0.05.

recognized by 5C6 and 6H7 are far away from the above mentioned, and no overlap between them was observed, which is conducive to form optimal antibody pairs for S protein detection.

It has been reported that SARS-CoV-2 S protein undergoes conformational movement involving RBD lying down and standing up, which benefits SARS-CoV-2 entry into host cells, immune escape and might interfere with exposure of some antigenic sites (Fig. S4). In terms of SARS-CoV-2 unique antigenic sites, sites targeted by 6G9 and 5C6 can be accessible in both standing up RBD and lying down RBD, in contrast, the antigenic site recognized by 5C4 can be fully exposed for binding, only when S protein is open with RBD standing up (Fig. 6A and B). In addition, the S protein amino-acid sequence of SARS-CoV-2 and SARS-CoV are similar (identity: ~77%), which provides molecular basis for the elicitation of cross-reactive mAbs in COVID-19 patients. In this study, cross-reactive antibodies (6G3, 4D10 and 6H7) recognized conserved residues of RBD between SARS-CoV-2 and SARS-CoV, revealing that these mAbs can give a full play to the advantage of simultaneous detection of these two types of coronavirus (Fig. 6A). In terms of conserved antigenic sites, sites for 6G3 and 4D10 in closed S protein were buried by adjacent lying down RBD, and 6G3 antigenic site was more accessible than 4D10 epitope in standing up RBD, which supported the better detection performance of 6G3 as detection antibody than 4D10 (Fig. 6C). 6H7 antigenic site can be fully exposed without influence by S protein conformational changes, so that 6H7 could more efficiently capture S protein of SARS-CoV than 6G3.

Additionally, we wonder whether 6H7 and 6G3 could be resistant to mutations of SARS-CoV-2 VOCs. The antigenic sites targeted by 6H7 and 6G3 were highly conserved among *Sarbecoviruses*, including SARS-CoV-2 VOCs (Fig. 6D). Then, the binding activities of 6H7 and 6G3 to VOCs were further detected using RBD proteins captured in plates. The results demonstrated that these two cross-reactive antibodies effectively bind to VOCs, including Omicron variant (Fig. 6E-F and Fig. S5), indicating that 6H7 and 6G3 antibody pair can play an important role in detection of SARS-CoV-2 VOCs. In summary, these results demonstrated the reason why 6H7-based antibody pairs showed remarkable detection performance and the potential of 6H7–6G3 antibody pair in broad detection of SARS-CoV and SARS-CoV-2 (including VOCs).

4. Discussion

Effective diagnostic is the frontline strategy for defeating infection outbreaks, such as COVID-19. Antigen detection methods are the important complementary detection methods for RT-PCR, due to advantages of simplicity and speed. For enveloped virus including coronavirus, transmembrane spike proteins are responsible for receptor

attachment, membrane fusion and entrance into host cells (Benton et al., 2020; Coultas, Smyth, and Openshaw, 2019; Ke et al., 2020; Kirchdoerfer et al., 2016; Wrapp et al., 2020). In this series of processes, the conformation of spike protein will change significantly. For instance, RSV fusion (F) protein, a type I fusion protein, can rearrange from a metastable prefusion conformation to a stable postfusion conformation, which causes some key antigenic sites to be exposed only in certain conformations (Magro et al., 2012; McLellan et al., 2011; Swanson et al., 2011; Walsh and Hruska, 1983). In terms of SARS-CoV-2 (or SARS-CoV), S proteins also represent diverse conformation, involving closed state and opening state. RBDs lying down is characteristic of closed conformation of S protein, which results in inaccessibility of some neutralizing antigenic sites and is conducive to immune escape (Ke et al., 2020; Kirchdoerfer et al., 2016; Piccoli et al., 2020; Wrapp et al., 2020). The difficulty of utilizing transmembrane spike proteins for diagnosis is caused by conformational complexity, which limits the development of diagnostic antigen kits (Kruttsagen et al., 2020; Qian et al., 2020). Therefore, due to conformational complexity of transmembrane spike proteins, consideration of multiple factors, including relative spatial position of antibodies, exposure and conservation of antigenic sites, antibody affinity and even presence of competitive antibodies in clinical samples, can contribute to screen effective antibody pairs for diagnosis of enveloped virus infection.

Due to the instability of SARS-CoV-2 S protein conformation, some antigenic sites may be accessible just in the opening state of S protein, which limits the binding of corresponding mAbs (Barnes et al., 2020). Similar to antigenic sites for 6G3 and 4D10, the site recognized by 5C4 is accessible just in the opening state of S protein, which might further influence detection capability of these candidate mAbs (Piccoli et al., 2020). In contrast, SARS-CoV-2 S protein either in opening state or in closed state, 6H7, 5C6 and 6G9 can efficiently recognize corresponding antigenic sites. As 6H7 neutralizes pseudovirus SARS-CoV-2 without blocking S protein binding to ACE2, it is inferred that 6H7 might significantly interfere with conformational change of S protein that is necessary for virus entrance into host cells (data not shown). Therefore, we speculate that conformation transition of S protein caused by 6H7 binding could provoke exposure of antigenic sites recognized by 6G3, which provides the theoretical basis of determining 6H7 as the detecting antibody. Additionally, the higher sensitivity of 6H7-based sandwich ELISA compared to ACE2-based lateral flow immunoassay also benefits from the conformation transition induced by 6H7 binding (Lee et al., 2021).

Furthermore, it is remarkable that the presence of competitive antibodies in samples including serum and nasopharyngeal swabs can influence the detection capacity of antibody pairs, due to the formation of

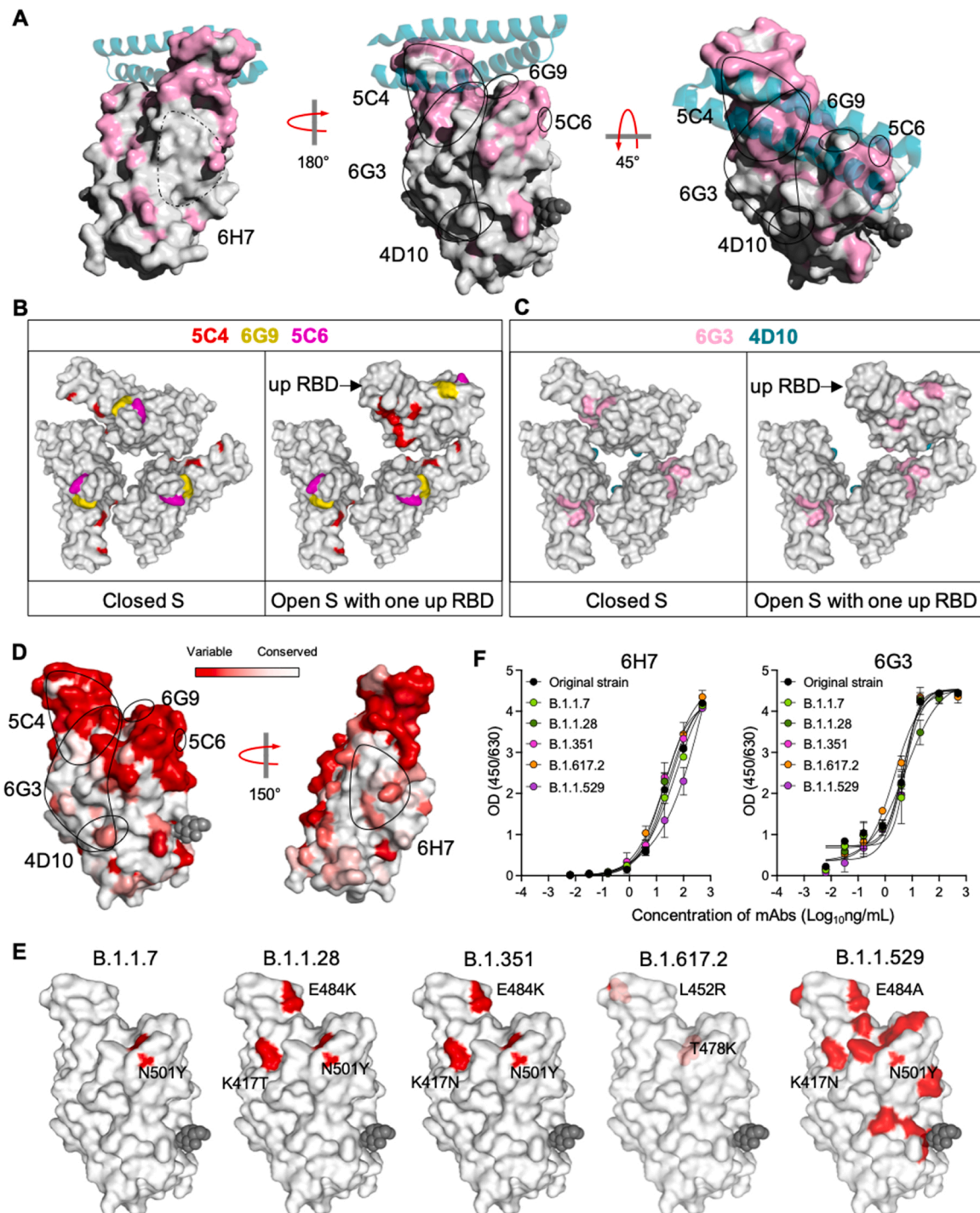


Fig. 6. Identification of epitopes recognized by candidate mAbs. (A) Residues different from SARS-CoV are shown on SARS-CoV-2 RBD by pink, and epitopes recognized by each candidate mAbs are shown as black outline. The glycan at position N343 is rendered as black spheres and ACE2 (S19-P84) as blue cartoon. (B) For 5C4, 6G9 and 5C6, accessibility analysis of corresponding epitopes on either standing-up RBD or lying-down RBD of S protein. Red, yellow and purple denote epitopes for 5C4, 6G9 and 5C6 on RBD of S protein, respectively (PDB code: 6VYB). (C) Accessibility analysis of epitopes for 6G3 and 4D10 (in pink and blue, respectively) on either standing-up RBD or lying-down RBD of S protein. (D) Conservation analysis of antigenic sites-directed by candidate mAbs using sequences including SARS-CoV-2 ($n = 2216,010$) and other *Sarbecoviruses* ($n = 80$). Deeper white indicates more conserved. (E) The spatial position of mutations on RBD domain of SARS-CoV-2 variants of concern. Red indicates the mutations. (F) The binding activity of 6H7 and 6G3 with S proteins of SARS-CoV-2 VOCs. These 2 mAbs were serially diluted to different concentrations and incubated in microwell plate coated with RBD protein of dominant variants for 30 min. Then the optical density was measured at 450 nm with a reference wavelength of 630 nm. The curve was analyzed by nonlinear regression (four-parameter).

immune complex with adverse effect. As antibodies derived from VH3-53/66 germline, display the native binding capability to SARS-CoV-2 RBD, such class antibodies contribute to form immunodominance in SARS-CoV-2-infected patients (Yuan et al., 2020). Hence,

detection capacity of 5C4, also encoded by VH3-53, will be reduced due to the stiff competition with such immunodominant antibodies, indicating that such mAbs, encoded by VH3-53/66 germline, are not suitable for diagnosis of COVID-19.

Another important issue that interferes S protein as suitable indicator for SARS-CoV-2 detection is the genetic variability and mutation rate. With the continuous spread of COVID-19 pandemic, a large number of SARS-CoV-2 variants appeared, then there is a growing concern that whether these new variants could impair the reliability of detection methods targeting S protein (Cerutti et al., 2021; Khateeb, Li, and Zhang, 2021; Korber et al., 2020; McCallum et al., 2021). For many SARS-CoV-2 VOCs, such as B.1.1.7 (Alpha), B.1.351 (Beta), B.1.1.28 (Gamma), B.1.617.2 (Delta) and B.1.1.529 (Omicron), RBD mutations mainly reside in the ACE2-binding site (known as the receptor-binding motif-RBM) that is a key target of functional antibodies. Since the antigenic sites identified by 6H7 and 6G3 are far from RBM and highly conserved between SARS-CoV-2 and SARS-CoV and even among SARS-CoV-2 variants, the ability of these two mAbs binding to S protein of variants can be guaranteed to the maximum extent, indicating that the 6H7–6G3 antibody pair can still play a reliable role in detecting emerging SARS-CoV-2 variants in the future.

Additionally, the antigen detection using ELISA remains disadvantage in the massive diagnostic and need for rapid results. In the contrast, lateral flow immunoassay (LFA) as rapid antigen diagnostic tests is cheap, fast (20–30 min) and easy-to-use tools without requirement for specific laboratory supplies, and even could generate test results at home. Next, we would develop 6H7–6G3 antibody pair as LFA, which is a promising tool in controlling COVID-19 pandemic.

In summary, due to the conformational complexity of SARS-CoV-2 S protein, multiple aspects have to be considered for optimal antibody pairs screening. In the end, 6H7–6G3 antibody pair was identified for sandwich ELISA. Considering the conserved antigenic sites targeted by 6H7 and 6G3, antigen detection methods using these 2 mAbs could play an important role in containing COVID-19 pandemic, even caused by emerging COVs. Moreover, this study also provides a significant guide to the screening of antibody pairs detecting other pathogens antigen with complex conformation.

Ethics approval

This article does not contain any studies with animal or human participants performed by any of the authors.

Data availability

All data generated or analyzed during this study are included in this article.

CRedit authorship contribution statement

S.W., Y.W., T.Z., Z.Z. and N.X. contributed to the experimental design. S.W., Y.W., Y.W., T.Z., Z.Z. and N.X. participated in discussion and interpretation of the results. S.G., H.S., X.C., H.Q., and Y.Y. conducted experiments. Z.C., D.Y., X.L., J.Z., Y.Z. and C.L. analyzed data. All authors approved the final version.

Declaration of Competing Interest

No potential conflict of interest was reported by the author(s).

Acknowledgements

This work was supported by the National Natural Science Foundation of China [grant number 82041038], the National Key Research and Development Program of China [grant number 2020YFC0842600] and the Science and Technology Major Project of Fujian [grant number 2020YZ014001].

Appendix A. Supporting information

Supplementary data associated with this article can be found in the online version at doi:10.1016/j.jviromet.2022.114597.

References

- Barnes, C.O., Jette, C.A., Abernathy, M.E., Dam, K.A., Esswein, S.R., Gristick, H.B., Maluyutin, A.G., Sharaf, N.G., Huey-Tubman, K.E., Lee, Y.E., Robbiani, D.F., Nussenzweig, M.C., West Jr., A.P., Bjorkman, P.J., 2020. SARS-CoV-2 neutralizing antibody structures inform therapeutic strategies. *Nature* 588, 682–687.
- Ben-Ami, R., Klochendler, A., Seidel, M., Sido, T., Gurel-Gurevich, O., Yassour, M., Meshorer, E., Benedek, G., Fogel, I., Oiknine-Djian, E., Gertler, A., Rotstein, Z., Lavi, B., Dor, Y., Wolf, D.G., Salton, M., Drier, Y., Hebrew University-Hadassah, C.-D. T., 2020. Large-scale implementation of pooled RNA extraction and RT-PCR for SARS-CoV-2 detection. *Clin. Microbiol. Infect.* 26, 1248–1253.
- Benton, D.J., Gamblin, S.J., Rosenthal, P.B., Skehel, J.J., 2020. Structural transitions in influenza haemagglutinin at membrane fusion pH. *Nature* 583, 150–153.
- Cameroni, E., Bowen, J.E., Rosen, L.E., Saliba, C., Zepeda, S.K., Culp, K., Pinto, D., VanBlargan, L.A., De Marco, A., di Iulio, J., Zatta, F., Kaiser, H., Noack, J., Farhat, N., Czudnochowski, N., Havenar-Daughton, C., Sprouse, K.R., Dillen, J.R., Powell, A.E., Chen, A., Maher, C., Yin, L., Sun, D., Soriaga, L., Bassi, J., Silacci-Fregni, C., Gustafsson, C., Franko, N.M., Logue, J., Iqbal, N.T., Mazzei, L., Geffner, J., Griffantini, R., Chu, H., Gori, A., Riva, A., Giannini, O., Ceschi, A., Ferrari, P., Cippa, P.E., Franzetti-Pellanda, A., Garzoni, C., Halfmann, P.J., Kawaoka, Y., Hebrner, C., Purcell, L.A., Piccoli, L., Pizzuto, M.S., Walls, A.C., Diamond, M.S., Telenti, A., Virgin, H.W., Lanzavecchia, A., Snell, G., Veesler, D., Corti, D., 2022. Broadly neutralizing antibodies overcome SARS-CoV-2 Omicron antigenic shift. *Nature* 602, 664–670.
- Cao, Y., Wang, J., Jian, F., Xiao, T., Song, W., Yisimayi, A., Huang, W., Li, Q., Wang, P., An, R., Wang, J., Wang, Y., Niu, X., Yang, S., Liang, H., Sun, H., Li, T., Yu, Y., Cui, Q., Liu, S., Yang, X., Du, S., Zhang, Z., Hao, X., Shao, F., Jin, R., Wang, X., Xiao, J., Wang, Y., Xie, X.S., 2022. Omicron escapes the majority of existing SARS-CoV-2 neutralizing antibodies. *Nature* 602, 657–663.
- Cerutti, G., Guo, Y.C., Zhou, T.Q., Gorman, J., Lee, M., Rapp, M., Reddem, E.R., Yu, J., Bahna, F., Bimela, J., Huang, Y.X., Katsamba, P.S., Liu, L.H., Nair, M.S., Rawi, R., Olia, A.S., Wang, P.F., Zhang, B.S., Chuang, G.Y., Ho, D.D., Sheng, Z.Z., Kwong, P.D., Shapiro, L., 2021. Potent SARS-CoV-2 neutralizing antibodies directed against spike N-terminal domain target a single supersite. *Cell Host Microbe* 29, 819–833.
- Coults, J.A., Smyth, R., Openshaw, P.J., 2019. Respiratory syncytial virus (RSV): a scourge from infancy to old age. *Thorax* 74, 986–993.
- Ke, Z., Otonari, J., Qu, K., Cortese, M., Zila, V., McKeane, L., Nakane, T., Zivanov, J., Neufeldt, C.J., Cerikan, B., Lu, J.M., Peukes, J., Xiong, X., Krausslich, H.G., Scheres, S.H.W., Bartenschlager, R., Briggs, J.A.G., 2020. Structures and distributions of SARS-CoV-2 spike proteins on intact virions. *Nature* 588, 498–502.
- Khateeb, J., Li, Y., Zhang, H., 2021. Emerging SARS-CoV-2 variants of concern and potential intervention approaches. *Crit. Care* 25, 244–251.
- Kim, D., Lee, J.Y., Yang, J.S., Kim, J.W., Kim, V.N., Chang, H., 2020. The Architecture of SARS-CoV-2 Transcriptome. *Cell* 181, 914–921.
- Kirchdoerfer, R.N., Cottrell, C.A., Wang, N., Pallesen, J., Yassine, H.M., Turner, H.L., Corbett, K.S., Graham, B.S., McLellan, J.S., Ward, A.B., 2016. Pre-fusion structure of a human coronavirus spike protein. *Nature* 531, 118–121.
- Korber, B., Fischer, W.M., Gnanakaran, S., Yoon, H., Theiler, J., Abfalterer, W., Hengartner, N., Giorgi, E.E., Bhattacharya, T., Foley, B., Hastie, K.M., Parker, M.D., Partridge, D.G., Evans, C.M., Freeman, T.M., de Silva, T.L., McDanal, C., Perez, L.G., Tang, H.L., Moon-Walker, A., Whelan, S.P., LaBranche, C.C., Saphire, E.O., Montefiori, D.C., Grp, S.C.-G., 2020. Tracking changes in SARS-CoV-2 spike: evidence that D614G increases infectivity of the COVID-19 virus. *Cell* 182, 812–827.
- Kruttgen, A., Cornelissen, C.G., Dreher, M., Hornef, M., Imohl, M., Kleines, M., 2020. Comparison of four new commercial serologic assays for determination of SARS-CoV-2 IgG. *J. Clin. Virol.* 128, 1–3.
- Lan, J., Ge, J., Yu, J., Shan, S., Zhou, H., Fan, S., Zhang, Q., Shi, X., Wang, Q., Zhang, L., Wang, X., 2020. Structure of the SARS-CoV-2 spike receptor-binding domain bound to the ACE2 receptor. *Nature* 581, 215–220.
- Lee, J.H., Choi, M., Jung, Y., Lee, S.K., Lee, C.S., Kim, J., Kim, J., Kim, N.H., Kim, B.T., Kim, H.G., 2021. A novel rapid detection for SARS-CoV-2 spike 1 antigens using human angiotensin converting enzyme 2 (ACE2). *Biosens. Bioelectron.* 171, 1–10.
- Lee, V.J., Chiew, C.J., Khong, W.X., 2020. Interrupting transmission of COVID-19: lessons from containment efforts in Singapore. *J. Travel. Med.* 27, 1–5.
- Li, D., Wang, D., Dong, J., Wang, N., Huang, H., Xu, H., Xia, C., 2020. False-negative results of real-time reverse-transcriptase polymerase chain reaction for severe acute respiratory syndrome coronavirus 2: role of deep-learning-based CT diagnosis and insights from two cases. *Korean J. Radiol.* 21, 505–508.
- Magro, M., Mas, V., Chappell, K., Vázquez, M., Cano, O., Luque, D., Terrón, M.C., Melero, J.A., Palomo, C., 2012. Neutralizing antibodies against the preactive form of respiratory syncytial virus fusion protein offer unique possibilities for clinical intervention. *Proc. Natl. Acad. Sci. U. S. A.* 109, 3089–3094.
- Mavrikou, S., Moschopoulou, G., Tsekouras, V., Kintziotis, S., 2020. Development of a portable, ultra-rapid and ultra-sensitive cell-based biosensor for the direct detection of the SARS-CoV-2 S1 spike protein antigen. *Sensors* 20, 3132–3138.
- McCallum, M., Marco, De Lempp, A., Tortorici, F., Pinto, M.A., Walls, D., Beltramello, A. C., Chen, M., Liu, A., Zatta, Z.M., Zepeda, F., di Iulio, S., Bowen, J., Montiel-Ruiz, J. E., Zhou, M., Rosen, J.Y., Bianchi, L.E., Guarino, S., Fregni, B., Abdelnabi, C.S., Foo, R., Rothlauf, S.Y.C., Bloyet, P.W., Benigni, L.M., Cameroni, F., Neyts, E.,

- Riva, J., Snell, A., Telenti, G., Whelan, A., Virgin, S.P.J., Corti, H.W., Pizzuto, M. S. D., Veessler, D., 2021. N-terminal domain antigenic mapping reveals a site of vulnerability for SARS-CoV-2. *Cell* 184, 2332–2347.
- McLellan, J.S., Yang, Y., Graham, B.S., Kwong, P.D., 2011. Structure of respiratory syncytial virus fusion glycoprotein in the postfusion conformation reveals preservation of neutralizing epitopes. *J. Virol.* 85, 7788–7796.
- Piccoli, L., Park, Y.J., Tortorici, M.A., Czudnochowski, N., Walls, A.C., Beltramello, M., Silacci-Fregni, C., Pinto, D., Rosen, L.E., Bowen, J.E., Acton, O.J., Jaconi, S., Guarino, B., Minola, A., Zatta, F., Sprugasci, N., Bassi, J., Peter, A., De Marco, A., Nix, J.C., Mele, F., Jovic, S., Rodriguez, B.F., Gupta, S.V., Jin, F., Piumatti, G., Lo Presti, G., Pellanda, A.F., Biggiogero, M., Tarkowski, M., Pizzuto, M.S., Cameroni, E., Havenar-Daughton, C., Smithey, M., Hong, D., Lepori, V., Albanese, E., Ceschi, A., Bernasconi, E., Elzi, L., Ferrari, P., Garzoni, C., Riva, A., Snell, G., Sallusto, F., Fink, K., Virgin, H.W., Lanzavecchia, A., Corti, D., Veessler, D., 2020. Mapping neutralizing and immunodominant sites on the SARS-CoV-2 spike receptor-binding domain by structure-guided high-resolution serology. *Cell* 183, 1024–1042.
- Poland, G.A., Ovsyannikova, I.G., Crooke, S.N., Kennedy, R.B., 2020. SARS-CoV-2 vaccine development: current status. *Mayo. Clin. Proc.* 95, 2172–2188.
- Qian, C.G., Zhou, M., Cheng, F.M., Lin, X.T., Gong, Y.J., Xie, X.B., Li, P., Li, Z.Y., Zhang, P.G., Liu, Z.J., Hu, F., Wang, Y., Li, Q., Zhu, Y., Duan, G.K., Xing, Y.T., Song, H.Y., Xu, W.F., Liu, B.F., Xia, F.Z., 2020. Development and multicenter performance evaluation of fully automated SARS-CoV-2 IgM and IgG immunoassays. *Clin. Chem. Lab. Med.* 58, 1601–1607.
- Relova, D., Rios, L., Acevedo, A.M., Coronado, L., Perera, C.L., Perez, L.J., 2018. Impact of RNA degradation on viral diagnosis: an understated but essential step for the successful establishment of a diagnosis network. *Vet. Sci.* 5, 1–13.
- Rogers, T.F., Zhao, F., Huang, D., Beutler, N., Burns, A., He, W.T., Limbo, O., Smith, C., Song, G., Woehl, J., Yang, L., Abbott, R.K., Callaghan, S., Garcia, E., Hurtado, J., Parren, M., Peng, L., Ramirez, S., Ricketts, J., Ricciardi, M.J., Rawlings, S.A., Wu, N. C., Yuan, M., Smith, D.M., Nemazee, D., Teijaro, J.R., Voss, J.E., Wilson, I.A., Andrabi, R., Briney, B., Landais, E., Sok, D., Jardine, J.G., Burton, D.R., 2020. Isolation of potent SARS-CoV-2 neutralizing antibodies and protection from disease in a small animal model. *Science* 369, 956–963.
- Swanson, K.A., Settembre, E.C., Shaw, C.A., Dey, A.K., Rappuoli, R., Mandl, C.W., Dormitzer, P.R., Carfi, A., 2011. Structural basis for immunization with postfusion respiratory syncytial virus fusion F glycoprotein (RSV F) to elicit high neutralizing antibody titers. *Proc. Natl. Acad. Sci. U. S. A.* 108, 9619–9624.
- Walls, A.C., Park, Y.J., Tortorici, M.A., Wall, A., McGuire, A.T., Veessler, D., 2020. Structure, function, and antigenicity of the SARS-CoV-2 spike glycoprotein. *Cell* 181, 281–292.
- Walsh, E.E., Hruska, J., 1983. Monoclonal antibodies to respiratory syncytial virus proteins: identification of the fusion protein. *J. Virol.* 47, 171–177.
- Wang, S., Qiu, Z.Y., Hou, Y.N., Deng, X.Y., Xu, W., Zheng, T.T., Wu, P.H., Xie, S.F., Bian, W.X., Zhang, C., Sun, Z.W., Liu, K.P., Shan, C., Lin, A.F., Jiang, S.B., Xie, Y.H., Zhou, Q., Lu, L., Huang, J., Li, X., 2021a. AXL is a candidate receptor for SARS-CoV-2 that promotes infection of pulmonary and bronchial epithelial cells. *Cell Res.* 31, 126–140.
- Wang, S., Wu, D., Xiong, H., Wang, J., Tang, Z., Chen, Z., Wang, Y., Zhang, Y., Ying, D., Lin, X., Liu, C., Guo, S., Tian, W., Lin, Y., Zhang, X., Yuan, Q., Yu, H., Zhang, T., Zheng, Z., Xia, N., 2021b. Quantitative Analysis Of Conserved Sites on the SARS-CoV-2 receptor-binding domain to promote development of universal SARS-like coronavirus vaccines. *bioRxiv* 2021, 439161, 04.10.
- Watanabe, Y., Allen, J.D., Wrapp, D., McLellan, J.S., Crispin, M., 2020. Site-specific glycan analysis of the SARS-CoV-2 spike. *Science* 369, 330–333.
- Wen, G.P., Tang, Z.M., Yang, F., Zhang, K., Ji, W.F., Cai, W., Huang, S.J., Wu, T., Zhang, J., Zheng, Z.Z., Xia, N.S., 2015. A valuable antigen detection method for diagnosis of acute hepatitis E. *J. Clin. Microbiol.* 53, 782–788.
- Wrapp, D., Wang, N., Corbett, K.S., Goldsmith, J.A., Hsieh, C.L., Abiona, O., Graham, B. S., McLellan, J.S., 2020. Cryo-EM structure of the 2019-nCoV spike in the prefusion conformation. *Science* 367, 1260–1263.
- Wu, F., Zhao, S., Yu, B., Chen, Y.M., Wang, W., Song, Z.G., Hu, Y., Tao, Z.W., Tian, J.H., Pei, Y.Y., Yuan, M.L., Zhang, Y.L., Dai, F.H., Liu, Y., Wang, Q.M., Zheng, J.J., Xu, L., Holmes, E.C., Zhang, Y.Z., 2020. A new coronavirus associated with human respiratory disease in China. *Nature* 579, 265–269.
- Xie, X., Zhong, Z., Zhao, W., Zheng, C., Wang, F., Liu, J., 2020. Chest CT for typical coronavirus disease 2019 (COVID-19) pneumonia: relationship to negative RT-PCR testing. *Radiology* 296, E41–E45.
- Xiong, H.L., Wu, Y.T., Cao, J.L., Yang, R., Liu, Y.X., Ma, J., Qiao, X.Y., Yao, X.Y., Zhang, B.H., Zhang, Y.L., Hou, W.H., Shi, Y., Xu, J.J., Zhang, L., Wang, S.J., Fu, B.R., Yang, T., Ge, S.X., Zhang, J., Yuan, Q., Huang, B.Y., Li, Z.Y., Zhang, T.Y., Xia, N.S., 2020. Robust neutralization assay based on SARS-CoV-2 S-protein-bearing vesicular stomatitis virus (VSV) pseudovirus and ACE2-overexpressing BHK21 cells. *Emerg. Microbes Infect.* 9, 2105–2113.
- Yuan, M., Liu, H., Wu, N.C., Lee, C.D., Zhu, X., Zhao, F., Huang, D., Yu, W., Hua, Y., Tien, H., Rogers, T.F., Landais, E., Sok, D., Jardine, J.G., Burton, D.R., Wilson, I.A., 2020. Structural basis of a shared antibody response to SARS-CoV-2. *Science* 369, 1119–1123.
- Zafrullah, M., Khursheed, Z., Yadav, S., Sahgal, D., Jameel, S., Ahmad, F., 2004. Acidic pH enhances structure and structural stability of the capsid protein of hepatitis E virus. *Biochem. Biophys. Res. Commun.* 313, 67–73.
- Zhang, L., Jackson, C.B., Mou, H., Ojha, A., Peng, H., Quinlan, B.D., Rangarajan, E.S., Pan, A., Vanderheiden, A., Suthar, M.S., Li, W., Izard, T., Rader, C., Farzan, M., Choe, H., 2020. SARS-CoV-2 spike-protein D614G mutation increases virion spike density and infectivity. *Nat. Commun.* 11, 6013–6021.
- Zhou, P., Yang, X.L., Wang, X.G., Hu, B., Zhang, L., Zhang, W., Si, H.R., Zhu, Y., Li, B., Huang, C.L., Chen, H.D., Chen, J., Luo, Y., Guo, H., Jiang, R.D., Liu, M.Q., Chen, Y., Shen, X.R., Wang, X., Zheng, X.S., Zhao, K., Chen, Q.J., Deng, F., Liu, L.L., Yan, B., Zhan, F.X., Wang, Y.Y., Xiao, G.F., Shi, Z.L., 2020. A pneumonia outbreak associated with a new coronavirus of probable bat origin. *Nature* 579, 270–273.
- Zhu, N., Zhang, D., Wang, W., Li, X., Yang, B., Song, J., Zhao, X., Huang, B., Shi, W., Lu, R., Niu, P., Zhan, F., Ma, X., Wang, D., Xu, W., Wu, G., Gao, G.F., Tan, W., China Novel Coronavirus, I., Research, T., 2020. A novel coronavirus from patients with pneumonia in China, 2019. *N. Engl. J. Med.* 382, 727–733.